# A New Ken-Ken Puzzle Pattern Based Reconfiguration Technique for Maximum Power Extraction in Partial Shaded Solar PV Array

**MURUGESAN PALPANDIAN[1], DAVID PRINCE WINSTON[2], (Member, IEEE), BALACHANDRAN PRAVEEN KUMAR[3], CHERUKURI SANTHAN KUMAR[4], THANIKANTI SUDHAKAR BABU[5,6], (Senior Member, IEEE), AND HASSAN HAES ALHELOU[7], (Senior Member, IEEE)**

[1]Department of Electrical and Electronics Engineering, Thamirabharani Engineering College, Tirunelveli 627358, India
[2]Department of Electrical and Electronics Engineering, Kamaraj College of Engineering and Technology, Madhurai 626001, India
[3]Department of Electrical and Electronics Engineering, Bharat Institute of Engineering and Technology, Hyderabad 501510, India
[4]Department of Electrical and Electronics Engineering, Lords Institute of Engineering and Technology, Hyderabad 500008, India
[5]Department of Electrical and Electronics Engineering, Chaitanya Bharathi Institute of Technology, Hyderabad 500075, India
[6]Department of Electrical and Electronics Engineering, Nisantasi University, 34398 Istanbul, Turkey
[7]School of Electrical and Electronic Engineering, University College Dublin (UCD), Dublin 4, D04 V1W8 Ireland

Corresponding authors: Hassan Haes Alhelou (alhelou@ieee.org) and Thanikanti Sudhakar Babu (sudhakarbabu66@gmail.com)

**ABSTRACT** Solar Photovoltaic array may often be subjected to partial shading, which may lead to uneven row current and creates local maximum power point on the power-voltage characteristics. One of the effective approaches to dilute the concentration of partial shading is the array reconfiguration technique. This study proposes a ken-ken puzzle-based reconfiguration technique for $4 \times 4$ total-cross-tied configuration to rearrange the position of modules within the array and to improve the maximum power under partial shading conditions. Further, the performance of the ken-ken puzzle arrangement is compared with the total-cross-tied configuration and existing reconfiguration techniques namely odd-even, Latin Square, and Sudoku reported in the literature. The performance of all these configurations is evaluated in terms of fill factor, mismatch loss, power loss, execution ratio, and performance enhancement ratio. The proposed ken-ken puzzle-based reconfiguration technique mitigates the occurrence of local maximum power point and eliminates the need for a complex algorithm to track the global maximum power point. The simulation result shows that the KK puzzle-based reconfiguration technique has obtained an improved PE of 10.85 % compared to TCT configuration, followed by LS, Sudoku, and OE. Also, the experimental result shows the effectiveness of the ken-ken in diluting the effects of partial shading when the rows of the photovoltaic array are shaded. The ken-ken puzzle-based reconfiguration technique reduces the complexity, maintenance and increases reliability, scalability of the PV array.

**INDEX TERMS** Shade dispersion, ken-ken puzzle pattern, global maximum power point, local maximum power point, and performance enhancement ratio.

## I. INTRODUCTION

The partial shading can occur in a photovoltaic (PV) module due to shading of nearby buildings, clouds, dust, and dirt, etc. The shaded modules consume power from the non-shaded modules and dissipate energy in the form of heat. Therefore, the bypass diodes are connected across the modules [1]–[3]. However, this introduces local maximum power point (LMPP) in power-voltage (P-V) characteristics, which misleads the maximum power point tracking

controller in tracking the global maximum power point (GMPP) [4]–[7].

One of the approaches used to dilute the concentration of partial shading on the PV array is the reconfiguration technique. The reconfiguration technique aims to distribute the effects of partial shading uniformly throughout the array to obtain the uniform row current. Hence, the maximum power point of the shaded and unshaded modules can be utilized. Since the effectiveness of the reconfiguration technique depends on the type and position of the partial shading. Hence, it is crucial to find out the favorable configuration to improve the GMPP under partial shading conditions (PSCs) [8], [9].

The author of [10] has conducted a comprehensive analysis of series, parallel, series-parallel, total-cross-tied (TCT), bridge link, and honeycomb configurations to find out the favorable configuration under the PSCs. This study indicates that TCT configuration has obtained superior performance under most of the PSCs. The author of [11] has conducted a comprehensive analysis of series, parallel, series-parallel, TCT, bridge link, and honeycomb configuration under PSCs. This study result shows that the TCT configuration is favorable for the symmetrical array and honeycomb configuration for the unsymmetrical array.

According to the previous research, the TCT configuration is a favorable configuration to improve the GMPP under the PSCs [12]. A major concern with the TCT configuration, if the modules connected in a row are shaded, results in the reduction of output current. Hence, it is vital to disperse the shade uniformly throughout the array to minimize the mismatch losses (ML).

The reconfiguration scheme can be categorized as (i) dynamic configuration and (ii) static configuration. In a dynamic reconfiguration scheme, the physical position of the modules is rearranged dynamically to improve the output power using switches, sensors, and controllers. The dynamic reconfiguration can be implemented by (i) electrical array reconfiguration, the modules are rearranged based on the incident irradiation and shading pattern. The reconfiguration algorithms are used to rearrange the position of the modules [13], [14]. (ii) Irradiation equivalence technique, in which the position of the modules are altered by employing complex switches and sensors to obtain the uniform row currents. The relocation of modules is based on the type of shading pattern, it eliminates the need for bypass diode. However, finding the appropriate configuration is difficult [15]. (iii) The adaptive reconfiguration technique consists of a fixed bank and an adaptive bank. The modules in the fixed bank are connected in TCT configuration and remain static, whereas the adaptive bank is reconfigurable by employing a switching matrix to obtain uniform row current [16]–[18]. The dynamic configuration requires algorithms, switching matrix, and sensors that increase the complexity in the case of a large-scale PV system and economically not feasible for the small-scale PV system.

A static configuration utilizes a pre-defined one-time reconfiguration scheme, in which the physical position of the module is rearranged without altering the electrical connections. Thus, the effects of partial shading are dispersed throughout the PV array. Therefore, the static interconnection scheme eliminates the need for complex algorithms, switching matrix, sensors, and auxiliary circuits. Sudoku [19], optimal Sudoku [20], Futoshiki [21], and magic square [22] proposed puzzle arrangements to disperse the effects of partial shading. One common drawback persists in these techniques; they cannot be extended to array size other than the proposed configurations. To resolve this issue zig-zag method [23], adjacent shift [24] and dominance square technique [25] involves both row and column-based displacement of modules. However, it increases the complexity of interconnections. The author of [26] proposed a column index technique, which is suitable for the symmetrical and asymmetrical PV array. This method involves a high computational burden to form the shade dispersion matrix.

The author of [27] proposed an odd-even (OE) puzzle arrangement for $4 \times 4$ TCT configuration to disperse the effects of partial shading throughout the array without altering the electrical connection. The OE puzzle pattern used in this study has altered the position of the modules by row and column-wise. The author has verified the performance of the OE puzzle arrangements in terms of maximum power, compared to the TCT configuration. The result shows that the OE puzzle arrangement has enhanced the output power and reduced the LMPP.

The author of [28] proposed a Latin square (LS) puzzle arrangement for a $4 \times 4$ TCT array to disperse the effects of partial shading throughout the array without altering the electrical connections. The author has evaluated the performance of the LS puzzle arrangement in terms of GMPP, power loss (PL), and fill factor (FF). The result shows that the LS puzzle arrangements have improved the GMPP and FF with minimum PL compared to the TCT for most of the PSCs.

The author of [29] proposed a two-step reconfiguration technique with a reduced number of switches compared to existing methods. The author has compared the performance of the Sudoku puzzle arrangement with the TCT configuration. The study result shows that the Sudoku puzzle pattern has performed superior under most of the PSCs.

Based on the observation from the papers [27]–[29], a few short-comings are observed: In [27], if any row or column is shaded, the modules are rearranged in two rows, thus the shade is not uniformly dispersed throughout the array. Further, the row and column-based module displacement increase the complexity of interconnection. In [28], the modules in the first column of the PV array (11, 21, 31, and 41) have remained unaltered. If the shadow falls on the 1st column of the array it will remain unaltered. Also, the modules connected in the 1st row of the PV array (11, 12, 13, and 14) are connected in the diagonal. If the shade occurs on the diagonal, after reconfiguration the shaded modules are displaced

in the 1st-row results in the reduction of the output current. In [29], the complex algorithm and matrix switches are used to rearrange the position of the modules within the array, which increases the cost and complexity of the system. Also, the row and column-based module displacement increase the complexity of interconnection. Hence, it increases the wire length and complexity of the system and causes additional PL.

From the literature, it is evident that the one-time reconfiguration technique is superior to the electric array reconfiguration. However, the complexity of the one-time reconfiguration technique should be reduced. On this note, this study proposes a ken-ken (KK) puzzle-based reconfiguration technique that suitably mitigates the computational burden, complexity and increases flexibility. The KK puzzle arrangement can effectively rearrange the position of the modules within the TCT array, to dilute the effects of partial shading without altering the electrical connection. Further, the performance of the KK configuration is compared with TCT and OE [27], LS [28], and Sudoku [29] puzzle arrangement (Fig.1). The performance of the proposed and existing reconfiguration techniques are evaluated in terms of FF, ML, PL, execution ratio (ER), and performance enhancement ratio (PE).
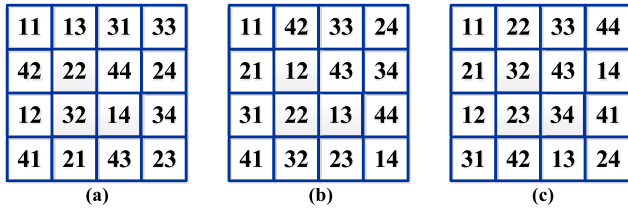
| 11 | 13 | 31 | 33 |
|----|----|----|----|
| 42 | 22 | 44 | 24 |
| 12 | 32 | 14 | 34 |
| 41 | 21 | 43 | 23 |

(a)

| 11 | 42 | 33 | 24 |
|----|----|----|----|
| 21 | 12 | 43 | 34 |
| 31 | 22 | 13 | 44 |
| 41 | 32 | 23 | 14 |

(b)

| 11 | 22 | 33 | 44 |
|----|----|----|----|
| 21 | 32 | 43 | 14 |
| 12 | 23 | 34 | 41 |
| 31 | 42 | 13 | 24 |

(c)

**FIGURE 1. Puzzle pattern: (a) OE (b) LS (c) Sudoku.**

The organization of the study is described as follows; In Section II, mathematical modeling of PV array is discussed. Section II. A describes the TCT configuration. In Section III.A, the Formation of the KK puzzle and pattern arrangement is discussed. In Section III.B, the Physical rearrangement of modules based on the KK puzzle patterns discussed. Section III.C describes the various shading pattern considered for simulation. Section III.D describes the performance parameter to analyze the performance of the PV array. Theoretical validation and simulation results are analyzed in Section IV. Section IV. A describes the comparison between various PV reconfiguration techniques. Section V describes the experimental verification along with a conclusion in Section V.

## II. MATHEMATICAL MODELING OF PV ARRAY

In this study, the single diode PV model is used because of its simplicity [30]. The single diode PV model is simulated in MATLAB Simulink environment for analyzing the performance of the PV array configuration. Fig.2. shows the equivalent circuit of the single diode PV cell. It consists of
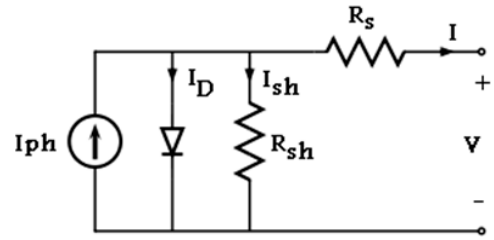
**FIGURE 2. Single diode PV cell.**

a current source, diode connected in anti-parallel with series ($R_s$) and parallel ($R_p$) resistance.

By applying Kirchhoff's current law, the current generated by the PV cell is given as

$$I = I_{ph} - I_D - I_{sh} \qquad (1)$$

where $I_{ph}$ is the photo-current generated by the incident irradiation, $I_D$ represents the non-linearity of the diode, $I_{sh}$ is the current flowing through the shunt resistor.

The current generated by the PV cell is given as [31]

$$I = I_{Ph} - I_o \left[ \exp\left( \frac{q(V + IR_s)}{akT} \right) - 1 \right] - \frac{V + IR_s}{R_{sh}} \qquad (2)$$

where $I_o$ is the saturation current of the diode, a is the ideality constant, q is the electron charge ($1.602 \times 10^{-19}$ C), k is the Boltzmann constant ($1.3806503 \times 10^{-23}$ J/K) and T is the cell temperature.

The PV module consists of series-connected cells ($N_{se}$) to form a module. The current flowing through the module is given as

$$I_m = I_{ph} - N_p I_o \left[ exp\left( \frac{q(V_m + R_s I_m)}{N_{se} akT} \right) - 1 \right] - \frac{V_m + R_s I_m N_{se}}{N_{se} R_{sh}} \qquad (3)$$

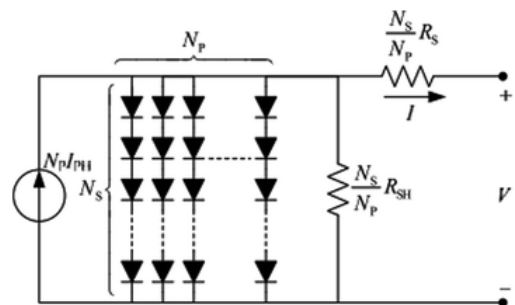where $I_m$ is the module current and $V_m$ is the module voltage ($V_m$) with $N_{se}$.

**FIGURE 3. Equivalent circuit of PV array.**

The PV modules consist of series-connected modules ($N_s$) and parallel-connected modules ($N_p$) to form a PV array as shown in Fig.3. The PV array current ($I_a$) in terms of array

| Electrical characteristics | Ratings |
|---|---|
| Maximum Power ($P_{max}$) | 200W |
| Open circuit voltage ($V_{oc}$) | 32.9V |
| The voltage at maximum power ($V_{mpp}$) | 26.3V |
| Short circuit current ($I_{sc}$) | 8.21A |
| Current at maximum power ($I_{mpp}$) | 7.61A |
| Number of cells connected in series ($N_s$) | 54 |

voltage ($V_a$) is given as

$$I_a = N_p I_{ph} - N_p I_o \left[ exp \left( \frac{q \left( V_a + R_s I_a \frac{N_s}{N_p} \right)}{N_s a k T} \right) - 1 \right] - \frac{V_a + R_s I_a \frac{N_s}{N_p}}{\frac{N_s}{N_p} R_{sh}} \quad (4)$$

The commercially available PV module Kyocera KC200GTis considered for the validation of simulation results in the MATLAB/Simulink environment. Table. 1 represents the specification of the PV module at standard test conditions (STC) at 1000W/m² and 25°C.
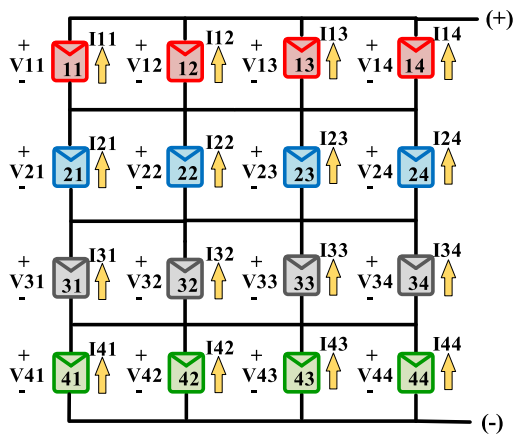


FIGURE 4. TCT PV array configuration.

## A. TOTAL-CROSS-TIEDPV ARRAY CONFIGURATION

In TCT configuration, the PV modules are connected in parallel to make ties and then all the ties are connected in series to form a string. Fig. 4. shows the 4×4 PV configuration consisting of 16 modules consisting of four rows and four columns. In each string, four modules are connected in parallel to form a row and each row are connected in series to form an array. The array current is the sum of current flowing the modules connected in parallel in a row [32]. During uniform irradiation conditions, the row current of the PV array is found to be equal. However, during the PSCs, the row current of the

PV array differs. Therefore, it is essential to calculate the row current to understand the severity of shade occurrences. The calculation of row current is used to determine the GMPP. The current is generated in the PV module at an irradiance condition.

$$I = \left( \frac{G}{G_{STC}} \right) I_m \quad (5)$$

By Kirchhoff'scurrent law, the current generated by each row can be expressed as [33]

$$I_{array} = \sum_{j=1}^{4} \left( I_{ij} - I(i+1)j \right) = 0 \quad i = 1, 2, 3, 4 \quad (6)$$

The array voltage can be is equal to the sum of the voltage across each row. By Kirchhoff'svoltage law, the voltage of the PV array is calculated as

$$V_{array} = \sum_{i=1}^{4} V_{mi} \quad (7)$$

The output power developed by the array can be expressed as

$$P_{array} = (V_{array})(I_{array}) = 16 V_m I_m \quad (8)$$

where G is the incident irradiation, $G_{STC}$ irradiation at STC, i is the number of a row of the array, and jis the number of columns of the array.

## III. METHODOLOGY

### A. FORMATION OFKEN-KEN PUZZLE AND PATTERN ARRANGEMENT

KK is a logic puzzle that belongs to the family of Sudoku. The KK puzzle has an m x n grid, in which the grid is separated into individual cages or groups of cages belong to different rows and columns. The size of the grid determines the logic number used in the puzzle. For the 4 × 4 grid, the numbers from 1 to 4 should be filled in the cage by an arithmetic operation such as addition, subtraction, multiplication, and division. Each cage is assigned with a digit and arithmetic operation. If the cage consists of only one square, the digit itself should be placed in the square. Each number should not repeat in a row or column. Fig. 5(a) shows the 4 × 4 puzzle considered for this study. The rules for solving the puzzle are as follows.

(i) In the second-row second column, the cage consists of digit 2 is assigned to one square, so this square is assigned with number 2.

(ii) In the third-row third column, the cage is assigned with digit 6 with an addition operation, since digit 2 already exists in the column so that column is filled with number 1, 3 and the remaining square is filled with number 2 as shown in Fig. 5(b).

(iii) In the first-row first column the cage consists of digit 48 with multiplication operator, the first column is filled with number 4, and the remaining square is filled with 1 and 3 as shown in Fig. 5(c).
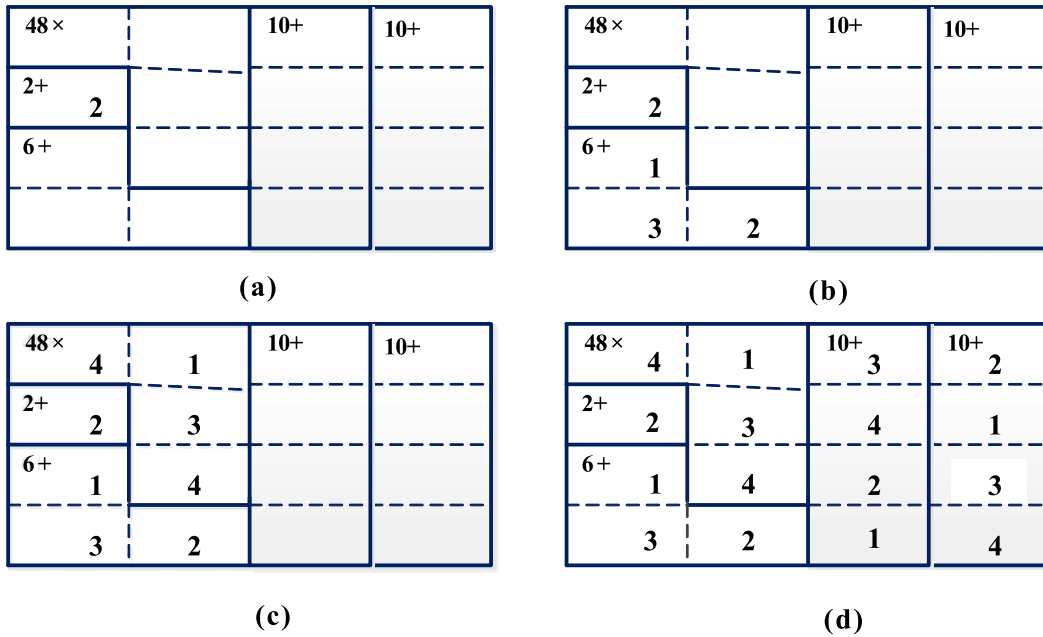
**FIGURE 5.** Formation of 4 × 4 KK puzzle (a). Arithmetic operation (b). Filling of the block with addition operation (2 and 6) (c). Filling of the block with multiplication operator 48 (d). Filling the two blocks with an arithmetic operation (10).

(iv) Similarly, the third and fourth column is filled by using the arithmetic operation as shown in Fig. 5. (d). Fig. 6. (a) shows obtained 4 × 4 KK puzzle and Fig. 6. (b) shows the pattern arrangement for the puzzle considered for further analysis.
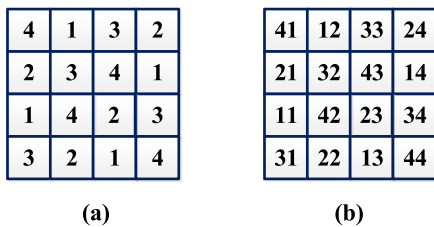


**FIGURE 6.** (a). KK puzzle and (b). KK puzzle arrangement.



**FIGURE 7.** Physical location (a). TCT array and (b). KK array.

type of shading pattern is applied on 4 × 4KK and existing puzzle arrangements and its effect of shade dispersion on the P-V characteristics of the PV array is analyzed.

### B. PHYSICAL REARRANGEMENT OF MODULES BASED ON KEN-KEN PUZZLE PATTERN

The puzzle arrangement of the KK configurations is represented in Fig. 6(b). In the puzzle pattern, the first digit represents the position of the module and the second digit refers to a column number. Fig. 7(a) shows the position of the modules in the TCT configuration and the rearrangement of TCT configuration based on the KK puzzle pattern without altering the electrical connection is shown in Fig. 7 (b).

### C. DESCRIPTION OF PARTIAL SHADING CONDITION

To validate the performance of the proposed and existing reconfiguration techniques, four types of shading patterns namely short narrow (SN), long narrow (LN), short wide (SW), and long wide (LW) are considered in this study. This
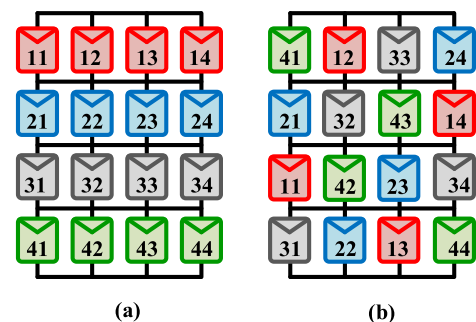
### 1) SHORT NARROW CONDITION

In SN condition, the PV array is subjected to three different irradiation levels such as 200 W/m$^2$, 600 W/m$^2$ for shaded modules, and 1000 W/m$^2$ for unshaded modules. Fig. 8 (a) represents the SN shading pattern on TCT configuration, the shading pattern and shade dispersion on KK arrangement is represented in Fig. 8 (b-c). Similarly, this type of shading pattern and shade dispersion is applied to the existing PV puzzle pattern.

### 2) LONG NARROW CONDITION

IIn LN condition, the PV array is subjected to four different irradiation levels as 400 W/m$^2$, 700 W/m$^2$, 900 W/m$^2$ for shaded modules, and 1000 W/m$^2$ for unshaded modules.
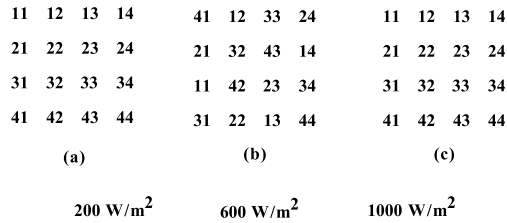
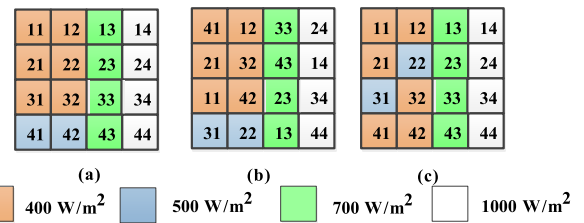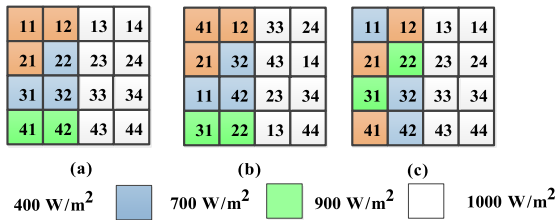**FIGURE 8.** Shading pattern for SN: (a). TCT arrangement (b-c). KK arrangement and shade dispersion.



**FIGURE 9.** Shading pattern for LN: (a). TCT arrangement (b-c). KK arrangement and shade dispersion.

Fig. 9 (a) represents the LN shading pattern on TCT configuration, the shading pattern and shade dispersion on KK arrangement is represented in Fig. 9 (b-c). In LN, the more number rows are shaded compared to SN.

### 3) SHORT WIDE CONDITION

In SW condition, the PV array is subjected to four different irradiation levels such as 400 W/m², 600 W/m², 700 W/m² for shaded modules, and 1000 W/m² for unshaded modules. Fig. 10 (a) represents the SW shading pattern on TCT configuration, the shading pattern and shade dispersion on KK arrangement is represented in Fig. 10 (b-c). In SW, the impact of partial shading on the PV array is high compared to SN and LN, which results in a high reduction in output power.
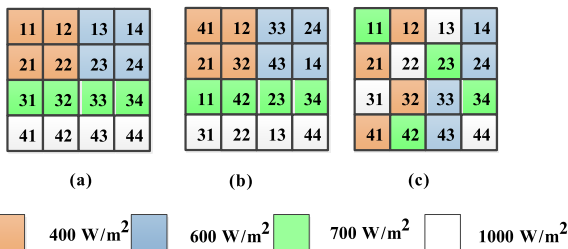


**FIGURE 10.** Shading pattern for SW: (a). TCT arrangement (b-c). KK arrangement and shade dispersion.

### 4) LONG WIDE CONDITION

In LW condition, the PV array is subjected to four different irradiation levels as 400 W/m², 500 W/m², 700 W/m² for shaded modules, and 1000 W/m² for unshaded modules. Fig. 11 (a) represents the LW shading pattern on TCT configuration, the shading pattern and shade dispersion on KK arrangement is represented in Fig. 11 (b-c). The impact of shading on the PV array is high compared to other shading patterns.



**FIGURE 11.** Shading pattern for LW: (a). TCT arrangement (b-c). KK arrangement and shade dispersion.

### D. PERFORMANCE PARAMETER UNDER PARTIAL SHADING CONDITIONS

The performance parameters are a clear indication of analyzing the performance of PV configuration under PSCs. The performance of the PV configurations is evaluated in terms of FF, ML, PL, ER, and PE. The performance parameters are elaborated in the subsequent subsections.

### 1) FILL FACTOR

Fill factor is the ratio GMPP at PSC to the product of open-circuit voltage($V_{oc}$) and short circuit current ($I_{sc}$) at STC.

$$\text{Fill factor} = \frac{V_{mpp}I_{mpp\,(at\,PSC)}}{V_{oc}I_{sc}} \quad (9)$$

### 2) MISMATCH LOSS

The partial shading leads to the GMPP and LMPP on the P-V characteristics

$$\text{Mismatch loss} = \text{Maximum power at STC}$$
$$-\text{Maximum power at the shaded condition} \quad (10)$$

### 3) POWER LOSS

Power loss is the ratio of the difference between maximum power at STC and PSC to the maximum power at STC.

$$\text{Power loss}$$
$$= \frac{\text{maximum power (STC) -maximum power }(PSC)}{\text{maximum power (STC)}} \times 100 \quad (11)$$

### 4) EXECUTION RATIO (%)

The execution ratio is the ratio of GMPP at the PSC and GMPP at STC. The execution ratio is defined as:

$$\text{Execution Ratio} = \frac{V_{mpp} \times I_{mpp(at\,PSC)}}{V_{mpp} \times I_{mpp\,(at\,STC)}} \times 100 \quad (12)$$

### 5) PERFORMANCE ENHANCEMENT RATIO COMPARED TO TCT (%)

Performance enhancement is defined as the ratio of the difference in power between GMPP at STC and PSCs.

$$\textit{Performance enhancement ratio}$$
$$= \frac{P_{GMPP}\,(OE,KK) - P_{GMPP}\,(TCT)}{P_{GMPP}\,(OE,KK)} \quad (13)$$

## IV. RESULTS AND DISCUSSION

In this study, the KK puzzle pattern-based reconfiguration technique is proposed for the $4 \times 4$ PV array to improve the GMPP under the PSCs. The performance of the KK reconfiguration is tested for SN, LN, SW, and LW PSCs. For each PSC, the row currents are theoretically calculated to locate the GMPP. To validate the effectiveness of the KK reconfiguration technique, its performance is compared with existing reconfiguration techniques like OE, LS, Sudoku, and TCT configuration in terms of FF, ML, PL, ER, and PE.

### A. SHORT NARROW CONDITION

The location of GMPPsare identified by calculating the current produced by each row of the PV array. The location of GMPP indicates the number of rows bypassed from the array to extract the maximum power. In the SN case, the shaded modules receive irradiation of 200 W/m$^2$, 600 W/m$^2$, and 1000 W/m$^2$ for unshaded modules as shown in Fig. 8. In this study, theoretical GMPPsarecalculated for TCT, OE, LS, Sudoku, and KK.

#### 1) ROW CURRENT CALCULATION FOR TCT CONFIGURATION

The row current for the 1$^{st}$ row of TCT configuration can be calculated as,

$$I_{row1} = \left(2 \times \left(\frac{200}{1000}\right) \times I_m\right) + \left(2 \times \left(\frac{1000}{1000}\right) \times I_m\right)$$
$$= 2.4 I_m \quad (14)$$

The row current for the 2$^{nd}$ row of TCT configuration can be calculated as,

$$I_{row2} = \left(2 \times \left(\frac{600}{1000}\right) \times I_m\right) + \left(2 \times \left(\frac{1000}{1000}\right) \times I_m\right)$$
$$= 3.2 I_m \quad (15)$$

The row current for the 3$^{rd}$ and 4$^{th}$ row of TCT configuration can be calculated as,

$$I_{row3} = I_{row4} = \left(4 \times \left(\frac{1000}{1000}\right) \times I_m\right) = 4 I_m \quad (16)$$

#### 2) ROW CURRENT CALCULATION FOR OE CONFIGURATION

The row current for the 1$^{st}$ row of OE configuration can be calculated as,

$$I_{row1} = \left(2 \times \left(\frac{200}{1000}\right) \times I_m\right) + \left(2 \times \left(\frac{1000}{1000}\right) \times I_m\right)$$
$$= 2.4 I_m \quad (17)$$

The row current for the 2$^{nd}$ row of OE configuration can be calculated as,

$$I_{row2} = \left(\left(\frac{600}{1000}\right) \times I_m\right) + \left(3 \times \left(\frac{1000}{1000}\right) \times I_m\right)$$
$$= 3.6 I_m \quad (18)$$

The row current for the 3$^{rd}$ row of OE configuration can be calculated as,

$$I_{row3} = \left(4 \times \left(\frac{1000}{1000}\right) \times I_m\right) = 4 I_m \quad (19)$$

The row current for the 4$^{th}$ row of OE configuration can be calculated as,

$$I_{row4} = \left(\left(\frac{600}{1000}\right) \times I_m\right) + \left(3 \times \left(\frac{1000}{1000}\right) \times I_m\right)$$
$$= 3.6 I_m \quad (20)$$

#### 3) ROW CURRENT CALCULATION FOR LS CONFIGURATION

The row current for the 1$^{st}$ row of LS configuration can be calculated as,

$$I_{row1} = \left(\left(\frac{200}{1000}\right) \times I_m\right) + \left(\left(\frac{600}{1000}\right) \times I_m\right)$$
$$+ \left(2 \times \left(\frac{1000}{1000}\right) \times I_m\right) = 3.2 I_m \quad (21)$$

The row current for the 2$^{nd}$ row of LS configuration can be calculated as,

$$I_{row2} = \left(\left(\frac{600}{1000}\right) \times I_m\right) + \left(3 \times \left(\frac{1000}{1000}\right) \times I_m\right)$$
$$= 3.6 I_m \quad (22)$$

The row current for the 3$^{rd}$ row of LS configuration can be calculated as,

$$I_{row3} = \left(4 \times \left(\frac{1000}{1000}\right) \times I_m\right) = 4 I_m \quad (23)$$

The row current for the 4$^{th}$ row of LS configuration can be calculated as,

$$I_{row4} = \left(\left(\frac{200}{1000}\right) \times I_m\right) + \left(3 \times \left(\frac{1000}{1000}\right) \times I_m\right)$$
$$= 3.2 I_m \quad (24)$$

#### 4) ROW CURRENT CALCULATION FOR SUDOKU CONFIGURATION

The row current for the 1$^{st}$ row of Sudoku configuration can be calculated as,

$$I_{row1} = \left(\left(\frac{200}{1000}\right) \times I_m\right) + \left(3 \times \left(\frac{1000}{1000}\right) \times I_m\right)$$
$$= 3.2 I_m \quad (25)$$

The row current for the 2$^{nd}$ row of Sudoku configuration can be calculated as,

$$I_{row2} = \left(\left(\frac{600}{1000}\right) \times I_m\right) + \left(\left(\frac{200}{1000}\right) \times I_m\right)$$
$$+ \left(2 \times \left(\frac{1000}{1000}\right) \times I_m\right) = 2.8 I_m \quad (26)$$

The row current for the 3$^{rd}$ row of Sudoku configuration can be calculated as,

$$I_{row3} = \left(\left(\frac{600}{1000}\right) \times I_m\right) + \left(3 \times \left(\frac{1000}{1000}\right) \times I_m\right)$$
$$= 3.6 I_m \quad (27)$$

The row current for the 4$^{th}$ row of Sudoku configuration can be calculated as,

$$I_{row4} = \left(4 \times \left(\frac{1000}{1000}\right) \times I_m\right) = 4 I_m \quad (28)$$

**TABLE 2.** Location of GMPPs in TCT, OE, LS, Sudoku, and KK configuration for PSCs.

| Shading pattern | | TCT $I_r \times I_m$ (A) | $V_r \times V_m$ (V) | $P_r \times V_m I_m$ (W) | | OE [27] $I_r \times I_m$ (A) | $V_r \times V_m$ (V) | $P_r \times V_m I_m$ (W) | | LS [28] $I_r \times I_m$ (A) | $V_r \times V_m$ (V) | $P_r \times V_m I_m$ (W) | | Sudoku [29] $I_r \times I_m$ (A) | $V_r \times V_m$ (V) | $P_r \times V_m I_m$ (W) | | KK $I_r \times I_m$ (A) | $V_r \times V_m$ (V) | $P_r \times V_m I_m$ (W) |
|---|---|---|---|---|---|---|---|---|---|---|---|---|---|---|---|---|---|---|---|---|
| SN | Ir1 | 2.4 | 4 | 9.6 | Ir1 | 2.4 | 4 | 9.6 | Ir1 | 2.8 | 4 | 11.2 | Ir2 | 2.8 | 4 | 11.2 | Ir1 | 3.2 | 4 | 12.8 |
| | Ir2 | 3.2 | 3 | 9.6 | Ir2 | 3.6 | 3 | 10.8 | Ir4 | 3.2 | 3 | 9.6 | Ir1 | 3.2 | 3 | 9.6 | Ir4 | 3.2 | 4 | 12.8 |
| | Ir3 | 4 | 2 | 8 | Ir4 | 3.6 | 3 | 10.8 | Ir2 | 3.6 | 2 | 7.2 | Ir3 | 3.6 | 2 | 7.2 | Ir2 | 3.6 | 2 | 7.2 |
| | Ir4 | 4 | 2 | 8 | Ir3 | 4 | 1 | 4 | Ir3 | 4 | 1 | 4 | Ir4 | 4 | 1 | 4 | Ir3 | 3.6 | 2 | 7.2 |
| LN | Ir1 | 2.8 | 4 | 11.2 | Ir1 | 2.5 | 4 | 10 | Ir1 | 3.1 | 4 | 12.4 | Ir2 | 2.5 | 4 | 10 | Ir1 | 3.1 | 4 | 12.4 |
| | Ir2 | 3.1 | 2 | 9.3 | Ir4 | 3.3 | 3 | 9.9 | Ir2 | 3.1 | 4 | 12.4 | Ir1 | 3.1 | 3 | 9.3 | Ir4 | 3.1 | 4 | 12.4 |
| | Ir3 | 3.4 | 2 | 6.8 | Ir2 | 3.6 | 2 | 7.2 | Ir4 | 3.3 | 2 | 6.6 | Ir3 | 3.6 | 2 | 7.2 | Ir2 | 3.3 | 2 | 9.9 |
| | Ir4 | 3.8 | 1 | 3.8 | Ir3 | 3.7 | 1 | 3.7 | Ir3 | 3.6 | 1 | 3.6 | Ir4 | 3.9 | 1 | 3.9 | Ir3 | 3.6 | 1 | 3.6 |
| SW | Ir1 | 2 | 4 | 8 | Ir1 | 2.2 | 4 | 8.8 | Ir1 | 2.5 | 4 | 10 | Ir2 | 2.5 | 4 | 10 | Ir1 | 2.7 | 4 | 10.8 |
| | Ir2 | 2 | 4 | 8 | Ir3 | 2.6 | 3 | 7.8 | Ir2 | 2.7 | 3 | 8.1 | Ir1 | 2.7 | 3 | 8.1 | Ir2 | 2.7 | 4 | 10.8 |
| | Ir3 | 2.8 | 2 | 5.6 | Ir2 | 3 | 2 | 6 | Ir4 | 2.7 | 3 | 8.1 | Ir3 | 2.7 | 3 | 8.1 | Ir3 | 2.7 | 4 | 10.8 |
| | Ir4 | 4 | 1 | 4 | Ir4 | 3 | 2 | 6 | Ir3 | 2.9 | 1 | 2.9 | Ir4 | 2.9 | 1 | 2.9 | Ir4 | 2.7 | 4 | 10.8 |
| LW | Ir1 | 2.5 | 4 | 10 | Ir1 | 1.9 | 4 | 7.6 | Ir1 | 2.5 | 4 | 10 | Ir2 | 2.2 | 4 | 8.8 | Ir3 | 2.5 | 4 | 10 |
| | Ir2 | 2.5 | 4 | 10 | Ir4 | 2.3 | 3 | 3.1 | Ir2 | 2.5 | 4 | 10 | Ir3 | 2.3 | 3 | 6.9 | Ir4 | 2.5 | 4 | 10 |
| | Ir3 | 2.5 | 4 | 10 | Ir2 | 2.9 | 2 | 5.8 | Ir3 | 2.6 | 2 | 5.2 | Ir1 | 2.5 | 2 | 5.0 | Ir1 | 2.6 | 2 | 5.2 |
| | Ir4 | 2.7 | 1 | 2.7 | Ir3 | 3.1 | 1 | 6.9 | Ir4 | 2.6 | 2 | 5.2 | Ir4 | 3.2 | 1 | 3.2 | Ir2 | 2.6 | 2 | 5.2 |

### 5) ROW CURRENT CALCULATION FOR KK CONFIGURATION

The row current for the 1$^{st}$ and 4$^{th}$ row of KK configuration can be calculated as,

$$I_{row1} = I_{row4}$$
$$= \left(1 \times \left(\frac{200}{1000}\right) \times I_m\right) + \left(3 \times \left(\frac{1000}{1000}\right) \times I_m\right)$$
$$= 3.2 I_m \qquad (29)$$

The row current for the 2$^{nd}$ and 3$^{rd}$ row of KK configuration can be calculated as,

$$I_{row2} = I_{row3}$$
$$= \left(1 \times \left(\frac{600}{1000}\right) \times I_m\right) + \left(3 \times \left(\frac{1000}{1000}\right) \times I_m\right)$$
$$= 3.6 I_m \qquad (30)$$

The theoretically calculated current, voltage, and power for each row of TCT, OE, LS, Sudoku, and KK configuration for SN condition are tabulated in Table 2. From Table. 2, it is observed that the KK configuration has produced a GMPP of 12.8 $V_m I_m$. The LS, Sudoku, OE, and TCT configuration follows the GMPP by 11.2 $V_m I_m$, 11.2 $V_m I_m$, 10.8 $V_m I_m$, and 9.6 $V_m I_m$ respectively. Further, the bypass diodes are provided to provide an alternate path for the flow of the current of the shaded modules.

In the existing reconfiguration techniques, two shades are dispersed on the same row even after reconfiguration. However, in the KK configuration, the effects of partial shadings are effectively dispersed throughout the array, which results in improved GMPP.Table.2 indicates the occurrence of LMPPon the P-V characteristics of TCT, OE, LS, Sudoku, and KK configuration. The KK reconfiguration technique has obtained only 2 LMPP on the P-V characteristics.

From the P-V characteristics (Fig.12), it is noticed that the TCT, OE, LS and Sudoku, and KK have obtained the GMPP of 2165 W, 2187 W, 2453 W, 2454 W, and 2653W respectively. From the Table. 3, it is understood that the KK has attained the maximum GMPP of 2653 W with FF, ML, PL, ER, and PE of 61.37 %, 547 W, 17.11 %, 82.89 %, and 18.37 % respectively.

### B. LONG NARROW CONDITION

The theoretically calculated current, voltage, and power of each row of TCT, OE, LS, Sudoku, and KK configurations for LN conditions are tabulated in Table 2. From Table 2, it is observed that the KK and LS configuration has produced a GMPP of 12.4 $V_m I_m$. The TCT, OE, and Sudoku configuration follow the GMPP by 11.2 $V_m I_m$, 10 $V_m I_m$ and 10 $V_m I_m$ respectively. From Table 2, it is clear that the KK and LS configuration has effectively dispersed the effects

| Shading pattern | Configuration | $I_a$ (A) | $V_a$ (V) | $P_a$ (W) | FF (%) | ML (W) | PL (%) | ER (%) | PE (%) | LMPP | Best Configuration |
|---|---|---|---|---|---|---|---|---|---|---|---|
| SN | TCT | 19.26 | 112.44 | 2165 | 50.10 | 1035 | 32.34 | 67.66 | NA | 2 | KK |
| | OE | 27.91 | 78.38 | 2187 | 50.61 | 1013 | 31.65 | 68.35 | 1.01 | 3 | |
| | LS | 22.51 | 108.98 | 2453 | 56.76 | 747 | 23.34 | 76.66 | 11.73 | 4 | |
| | Sudoku | 22.46 | 109.29 | 2454 | 56.79 | 746 | 23.30 | 76.70 | 11.78 | 4 | |
| | KK | 25.09 | 105.71 | 2653 | 61.37 | 547 | 17.11 | 82.89 | 18.37 | 2 | |
| LN | TCT | 22.11 | 109.73 | 2426 | 56.12 | 774 | 24.20 | 75.80 | NA | 4 | LS / KK |
| | OE | 20.14 | 110.72 | 2229 | 51.58 | 971 | 30.33 | 69.67 | -8.81 | 4 | |
| | LS | 24.21 | 105.71 | 2559 | 59.21 | 641 | 20.03 | 79.97 | 5.21 | 3 | |
| | Sudoku | 20.11 | 110.67 | 2226 | 51.50 | 974 | 30.44 | 69.56 | -8.97 | 4 | |
| | KK | 24.23 | 105.62 | 2559 | 59.21 | 641 | 20.03 | 79.97 | 5.21 | 3 | |
| SW | TCT | 15.75 | 108.96 | 1716 | 39.71 | 1484 | 46.37 | 53.63 | NA | 3 | KK |
| | OE | 17.51 | 109.92 | 1925 | 44.53 | 1275 | 39.85 | 60.15 | 10.84 | 3 | |
| | LS | 19.71 | 106.38 | 2097 | 48.52 | 1103 | 34.47 | 65.53 | 18.16 | 3 | |
| | Sudoku | 19.71 | 106.38 | 2097 | 48.52 | 1103 | 34.47 | 65.53 | 18.16 | 3 | |
| | KK | 20.41 | 104.84 | 2140 | 49.51 | 1060 | 33.13 | 66.88 | 19.81 | 1 | |
| LW | TCT | 19.43 | 103.48 | 2011 | 46.52 | 1189 | 37.17 | 62.83 | NA | 2 | TCT/LS/ KK |
| | OE | 15.27 | 109.87 | 1678 | 38.82 | 1522 | 47.56 | 52.44 | -19.83 | 4 | |
| | LS | 19.10 | 105.24 | 2011 | 46.52 | 1189 | 37.17 | 62.83 | 0.01 | 2 | |
| | Sudoku | 17.52 | 106.58 | 1867 | 43.20 | 1333 | 41.65 | 58.35 | -7.69 | 4 | |
| | KK | 19.40 | 103.66 | 2011 | 46.53 | 1189 | 37.16 | 62.84 | 0.01 | 2 | |



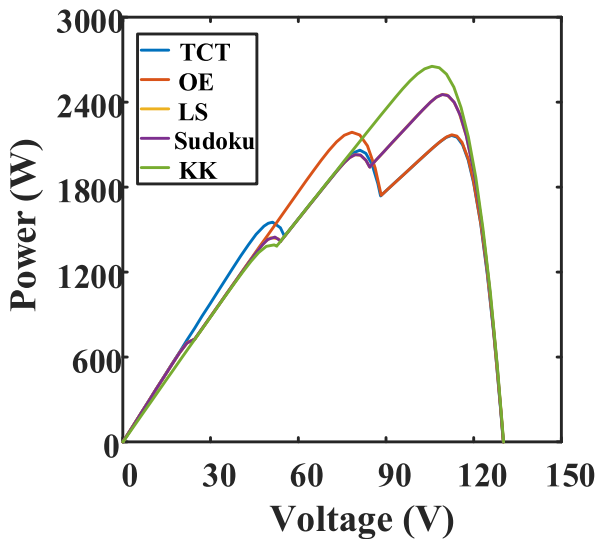**FIGURE 12.** P-V characteristics for SN condition.



**FIGURE 13.** P-V characteristics for LN condition.

of partial shading than the TCT, OE, and Sudoku configuration. Also, Table.2 indicates the occurrence of LMPPs on the P-V characteristics. The KK and LS configuration has obtained 3 LMPPs, whereas the 4 LMPPs have been obtained by the TCT, OE, and Sudoku configuration on the P-V characteristics.
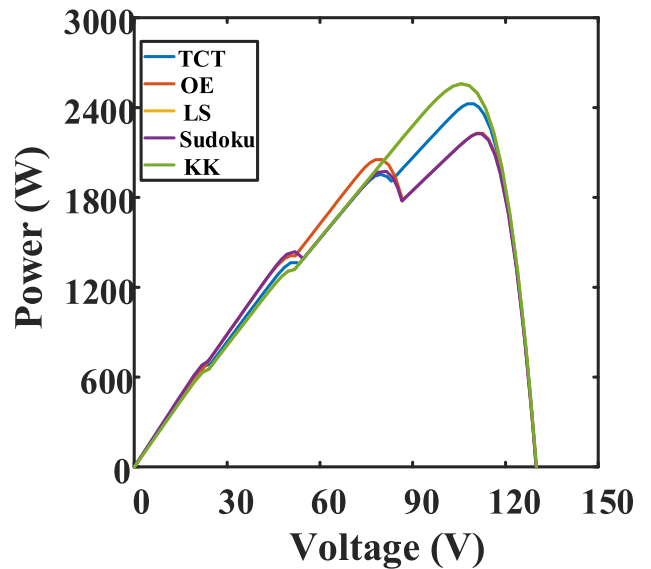
From the P-V characteristics (Fig.13), it is noticed that the TCT, OE, LS, Sudoku, and KK configuration has obtained GMPP of 2426 W, 2229 W, 2559 W, 2226 W, and 2559 W respectively. From the Table. 3, it is understood that the KK and LS configuration has attained the maximum GMPP

of 2559 W with FF, ML, PL, ER, and PE of 59.21 %, 641 W, 20.03 %, 79.97 %, and 5.27 %.

## C. SHORT WIDE CONDITION

The theoretically calculated current, voltage, and power of each row of TCT, OE, LS, Sudoku, and KK configuration for SW conditions are tabulated in Table 2. From Table 2, it is observed that the KK configuration has produced a GMPP of 10.8 $V_m I_m$. The LS, Sudoku, OE, and TCT configuration follows the GMPP by 10 $V_m I_m$, 10 $V_m I_m$, 8.8 $V_m I_m$, and 8 $V_m I_m$. From Fig. 10, it is clear that the KK configuration has dispersed effectively than the other configurations. In addition, Table.2 indicates the occurrence of LMPP on the P-V characteristics of TCT, OE, LS, Sudoku, and KK configurations. The KK configuration has obtained a single GMPP on the P-V characteristics.
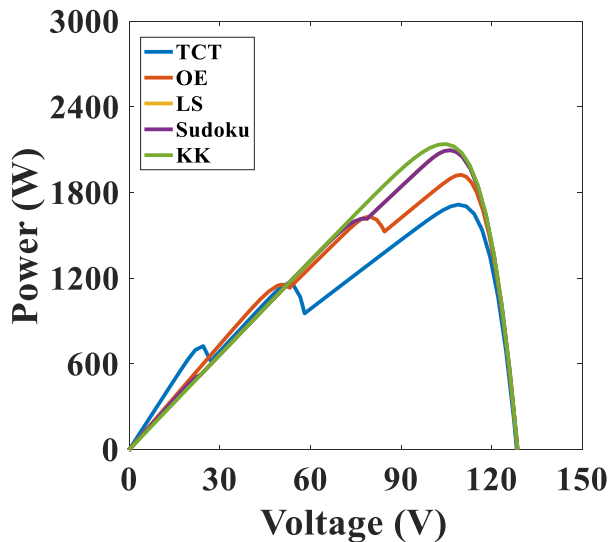


**FIGURE 14.** P-V characteristics for SW condition.

From the P-V characteristics (Fig.14), it is noticed that the TCT, OE, LS, Sudoku, and KK configuration has obtained GMPP of 1716 W, 1925 W, 2097 W, 2097 W, and 2140 W respectively. From the Table. 3, it is understood that the KK configuration has attained the maximum GMPP of 2140 W with FF, ML, PL, ER, and PE of 49.51 %, 1060 W, 33.13 %, 66.88 %, and 19.81 % respectively.

## D. LONG WIDE CONDITION

The theoretically calculated current, voltage, and power of each row of TCT, OE, LS, Sudoku, and KK configuration for LW conditions are tabulated in Table 2. From Table 2, it is observed that the KK, LS, and TCT configurations have obtained GMPP of 10 $V_m I_m$. The Sudoku and OE configuration follow the GMPP by8.8 $V_m I_m$ and 7.6 $V_m I_m$ respectively. In addition, Table. 2 indicates the occurrence of LMPP on the P-V characteristics. The KK, LS, and TCT configuration has obtained GMPP with 2 LMPPs on the P-V characteristics.
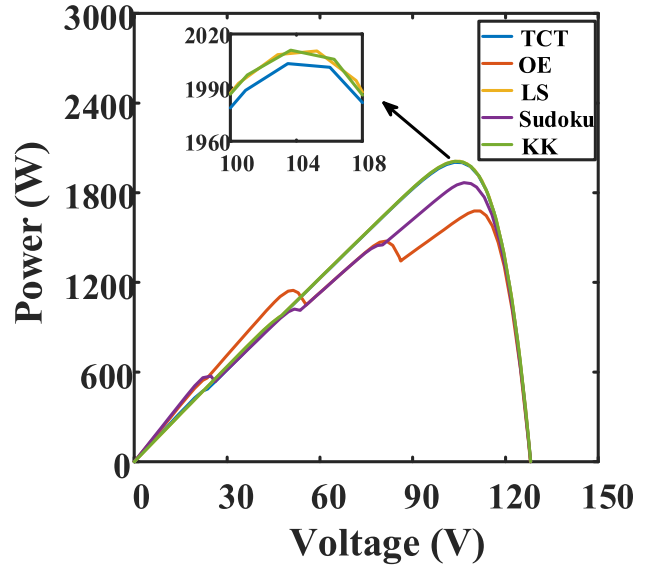


**FIGURE 15.** P-V characteristics for LW condition.

From the P-V characteristics (Fig.15), it is noticed that the TCT, OE, LS, Sudoku, and KK configuration has obtained maximum power of 2011 W, 1678 W, 2011 W, 1867 W, and 2011 W respectively. From the Table. 3, it is understood that the KK, LS, and TCT configuration has attained the maximum GMPP of 2011 W with FF, ML, PL, ER, and PE of 46.53 %, 1189 W, 37.16 %, 62.84 %, and 0.10 % respectively.

## E. COMPARISON BETWEEN VARIOUSPV RECONFIGURATION TECHNIQUES

The performance of the various reconfiguration techniques is compared in terms of displacement of modules in puzzle pattern, LMPP, PL, and PE. The PV modules are displaced on the column-wise in KK and LS, whereas row and column-wise in OE and Sudoku puzzle arrangements. The row and column-wise module displacement increases the wire length and complexity of the interconnections. In the SN condition, all the existing reconfiguration techniques have dispersed the shade on the three rows of the array. However, in the KK the shades are dispersed on the four rows of the array. Therefore, KK has obtained improved PE and a lesser number of LMPPs (Fig. 16) by dispersing the shade effectively compared to other configurations. In the LN condition, the shaded modules are dispersed effectively in the KK and LS compared to OE and Sudoku. In the SW condition, the KK configuration has obtained a single GMPP on the P-V characteristics. In the LW condition, KK, LS, and TCT have obtained improved PE with less LMPP compared to OE and Sudoku.

Fig. 17 shows the percentage power loss produced by the PV configuration under PSCs. The KK configuration has the least power loss compared to other configurations. The power loss is high in the SW and LW shading conditions, due to the increase in the occurrence of shade on the rows
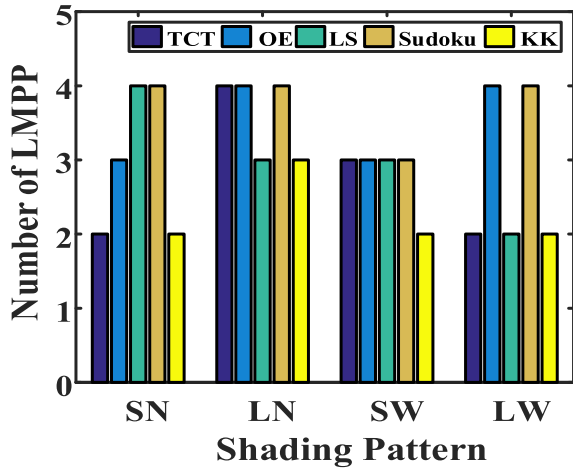
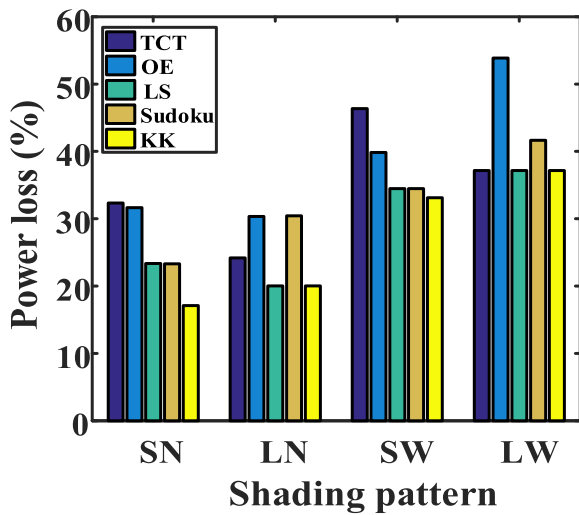**FIGURE 16.** The occurrence of LMPPs on-V characteristics.



**FIGURE 17.** Percentage power loss for PSCs.



**FIGURE 18.** Experimental verification of PV configurations.

**TABLE 4.** Experimental results.

| Types of Shading Pattern | Different types of configurations | | | | |
|---|---|---|---|---|---|
| | TCT | OE [27] | LS [28] | Sudoku [29] | KK |
| | Generated Power (W) | | | | |
| SN | 71 | 83 | 82 | 82 | 99 |
| LN | 77 | 72 | 97 | 73 | 97 |
| SW | 66 | 64 | 69 | 69 | 86 |
| LW | 80 | 56 | 80 | 59 | 80 |

of the PV array. The KK puzzle arrangements are found to superior followed by the LS in improving the GMPP under the considered PSCs.

## V. EXPERIMENTAL RESULTS

A detailed experimental study has been conducted using the proposed ken-ken puzzle-based reconfiguration technique of $4 \times 4$ PV array as shown in Fig. 18. The electrical parameters of the considered solar PV module are Power 10 W, $V_{oc} = 21.96$ V, $I_{sc} = 0.59$ A, $V_{mp} = 18.25$ V, $I_{mp} = 0.55$ A. The performance of the proposed and existing reconfiguration techniques, tested on different PSCs like SN, LN, SW and LW. The irradiation of the shaded modules are maintained as per the Fig. 8 – 11. The irradiation of the unshaded modules of SN, LN, SW, LW are 862 W/m$^2$, 832 W/m$^2$, 817 W/m$^2$ and 847 W/m$^2$ respectively. The experimental results of PSCs are reported in Table. 4.

For the SN condition, KK has generated maximum power of 99 W followed by the OE, LS, Sudoku and TCT by 83 W,

82 W, 82 W and 71 W. The KK has enhanced the maximum power by 28 % compared to TCT configuration. For the LN condition, KK and LS has generated maximum power of 97 W followed by TCT, Sudoku, OE by 77 W, 73 W and 72 W respectively. The KK has enhanced the maximum power by 20.61 % compared to TCT configuration. For the SW condition, KK has generated maximum power of 86 W followed by LS, Sudoku, TCT, OE by 69 W, 69 W, 66 W and 64 W respectively. The KK has enhanced the maximum power by 23.25 % compared to TCT configuration. For the LW condition, KK, TCT and LS has generated maximum power of 80 W followed by Sudoku and OE by 59 W and 56 W.

Overall, comparative analysis of the reconfiguration methods are reported in Table 5. From the Table 5, it is observed that the KK configuration has reduced the shading loss by dispersing the occurrence of the shade uniformly throughout the array and improves the power generation with reduced

**TABLE 5.** Overall comparative analysis of the reconfiguration methods.

| Parameter | TCT | OE [27] | LS [28] | Sudoku [29] | KK |
|---|---|---|---|---|---|
| Physical reconfiguration | √ | √ | √ | × | √ |
| Alter electrical connection | × | × | × | √ | × |
| Shade dispersion | Medium | Medium | Medium | Medium | High |
| Size of PV array | 4×4 | 4×4 | 4×4 | 4×4 | 4×4 |
| Sensor | × | × | × | √ | × |
| Switching matrix | × | × | × | √ | × |
| Reduce shading loss | Medium | Medium | Medium | Low | High |
| Increase generated power | Medium | Medium | Medium | Low | High |
| Complexity | Medium | Medium | Medium | High | Medium |
| Use intelligent algorithm | × | × | × | √ | × |
| Time consuming | High | High | High | High | Medium |
| Cost | Low | Low | Low | High | Low |
| Wire length | Medium | High | Medium | High | Medium |
| Maintenance | Medium | Medium | Medium | High | Medium |

complexity. The proposed KK configuration, relocates the physical position of the modules within the array without altering the electrical connection. Hence, it eliminates the need of complex algorithm, switching circuit and sensors. The KK and LS reconfiguration technique are found to be simple and economical compared to other OE and Sudoku.

## VI. CONCLUSION

In this study, a KK puzzle-based reconfiguration technique is proposed for a $4 \times 4$ TCT array to improve the GMPP under PSCs. The KK configuration relocates the position of the module column-wise within the TCT array without altering the electrical connections. The row current is derived for all the configurations to locate the theoretical GMPP. The investigation is carried out in MATLAB/Simulink environment. The performance of the KK configuration is compared with the TCT and existing configurations like OE, LS, and Sudoku configurations in terms of FF, ML, PL, ER, and PE. The simulation result of the study are as follows:

- For SN condition, the KK configuration has obtained PE of 18.37% followed by the Sudoku, LS, and OE configurations by 11.78 %, 11.73 %, and 1.01 % compared toTCT configuration.
- For the LN condition, the KK and LS configurations have PE of 5.21% followed by the OE and Sudoku configurations by −8.81 % and −8.97 % compared to TCT configuration.
- For SW condition, the KK configuration has a PE of 19.81 % followed by the LS, Sudoku, OE configurations by 18.16 %, 18.16%, and 10.86 % compared to TCT configuration.

- For LW conditions, the KK, LS, and TCT configurations have obtained the same output power and PE, followed by the Sudoku and OE configurations by −7.69% and −19.83 %.
- Overall, the KK configuration has obtained an improved PE of 10.85% followed by LS, Sudoku, and OE configurations by 8.78 %, 3.32 %, and −4.20 % compared to the TCT configuration under-considered PSCs.

Based on the simulation results, it is observed that the proposed KK puzzle arrangement can effectively disperse the shade throughout the array to improve GMPP with less number of LMPPs on the P-V characteristics. The KK is found to be an alternative for the existing puzzle-based reconfiguration techniques like OE, LS, Sudoku, and TCT configuration. The experimental verification shows the ability of the KK in diluting the effects of partial shading under the PSCs. The KK reconfiguration technique reduces the complexity, maintenance and increases reliability, scalability of the PV array. Therefore, the KK reconfiguration scheme economically viable for small scale and large scale, in which large array can be divided into a number of the small array.

## ACKNOWLEDGMENT

## REFERENCES

[1] D. Prince Winston, G. Karthikeyan, M. Pravin, O. JebaSingh, A. G. Akash, S. Nithish, and S. Kabilan, "Parallel power extraction technique for maximizing the output of solar PV array," *Sol. Energy*, vol. 213, pp. 102–117, Jan. 2021.

[2] D. P. Winston, S. Kumaravel, B. P. Kumar, and S. Devakirubakaran, "Performance improvement of solar PV array topologies during various partial shading conditions," *Sol. Energy*, vol. 196, pp. 228–242, Jan. 2020.

[3] D. Yousri, T. S. Babu, D. Allam, V. K. Ramachandaramurthy, E. Beshr, and M. B. Eteiba, "Fractional chaos maps with flower pollination algorithm for partial shading mitigation of photovoltaic systems," *Energies*, vol. 12, no. 18, p. 3548, Sep. 2019.

[4] D. P. Winston, "Efficient output power enhancement and protection technique for hot spotted solar photovoltaic modules," *IEEE Trans. Device Mater. Rel.*, vol. 19, no. 4, pp. 664–670, Dec. 2019.

[5] S. Obukhov, A. Ibrahim, A. A. Zaki Diab, A. S. Al-Sumaiti, and R. Aboelsaud, "Optimal performance of dynamic particle swarm optimization based maximum power trackers for stand-alone PV system under partial shading conditions," *IEEE Access*, vol. 8, pp. 20770–20785, 2020.

[6] A. Ali, K. Almutairi, S. Padmanaban, V. Tirth, S. Algarni, K. Irshad, S. Islam, M. H. Zahir, M. Shafiullah, and M. Z. Malik, "Investigation of MPPT techniques under uniform and non-uniform solar irradiation condition—A retrospection," *IEEE Access*, vol. 8, pp. 127368–127392, 2020.

[7] M. N. I. Jamaludin, M. F. N. Tajuddin, J. Ahmed, A. Azmi, S. A. Azmi, N. H. Ghazali, T. S. Babu, and H. H. Alhelou, "An effective salp swarm based MPPT for photovoltaic systems under dynamic and partial shading conditions," *IEEE Access*, vol. 9, pp. 34570–34589, 2021.

[8] A. S. Yadav, R. K. Pachauri, and Y. K. Chauhan, "Comprehensive investigation of PV arrays with puzzle shade dispersion for improved performance," *Sol. Energy*, vol. 129, pp. 256–285, May 2016.

[9] D. Yousri, T. S. Babu, S. Mirjalili, N. Rajasekar, and M. A. Elaziz, "A novel objective function with artificial ecosystem-based optimization for relieving the mismatching power loss of large-scale photovoltaic array," *Energy Convers. Manage.*, vol. 225, Dec. 2020, Art. no. 113385.

[10] F. Belhachat and C. Larbes, "Modeling, analysis and comparison of solar photovoltaic array configurations under partial shading conditions," *Sol. Energy*, vol. 120, pp. 399–418, Oct. 2015.

[11] R. Ramaprabha and B. L. Mathur, "A comprehensive review and analysis of solar photovoltaic array configurations under partial shaded conditions," *Int. J. Photoenergy*, vol. 2012, pp. 1–16, Feb. 2012.

[12] A. M. Ajmal, T. S. Babu, V. K. Ramachandaramurthy, D. Yousri, and J. B. Ekanayake, "Static and dynamic reconfiguration approaches for mitigation of partial shading influence in photovoltaic arrays," *Sustain. Energy Technol. Assessments*, vol. 40, Aug. 2020, Art. no. 100738.

[13] D. Prince Winston, K. Ganesan, P. K. B, D. Samithas, and C. B. Baladhanautham, "Experimental investigation on output power enhancement of partial shaded solar photovoltaic system," *Energy Sour. A, Recovery, Utilization, Environ. Effects*, pp. 1–17, Jun. 2020.

[14] T. S. Babu, D. Yousri, and K. Balasubramanian, "Photovoltaic array reconfiguration system for maximizing the harvested power using population-based algorithms," *IEEE Access*, vol. 8, pp. 109608–109624, 2020.

[15] G. Velasco-Quesada, F. Guinjoan-Gispert, R. Pique-Lopez, M. Roman-Lumbreras, and A. Conesa-Roca, "Electrical PV array reconfiguration strategy for energy extraction improvement in grid-connected PV systems," *IEEE Trans. Ind. Electron.*, vol. 56, no. 11, pp. 4319–4331, Nov. 2009.

[16] E. R. Sanseverino, T. N. Ngoc, M. Cardinale, V. Li Vigni, D. Musso, P. Romano, and F. Viola, "Dynamic programming and munkres algorithm for optimal photovoltaic arrays reconfiguration," *Sol. Energy*, vol. 122, pp. 347–358, Dec. 2015.

[17] M. Karakose, K. Murat, E. Akin, and K. S. Parlak, "A new efficient reconfiguration approach based on genetic algorithm in PV systems," in *Proc. IEEE 23rd Int. Symp. Ind. Electron. (ISIE)*, Jun. 2014, pp. 23–28.

[18] V. S. Bhadoria, R. K. Pachauri, S. Tiwari, S. P. Jaiswal, and H. H. Alhelou, "Investigation of different BPD placement topologies for shaded modules in a series-parallel configured PV array," *IEEE Access*, vol. 8, pp. 216911–216921, 2020.

[19] B. I. Rani, G. S. Ilango, and C. Nagamani, "Enhanced power generation from PV array under partial shading conditions by shade dispersion using su do ku configuration," *IEEE Trans. Sustain. Energy*, vol. 4, no. 3, pp. 594–601, Jul. 2013.

[20] M. Horoufiany and R. Ghandehari, "Optimization of the sudoku based reconfiguration technique for PV arrays power enhancement under mutual shading conditions," *Sol. Energy*, vol. 159, pp. 1037–1046, Jan. 2018.

[21] H. S. Sahu, S. K. Nayak, and S. Mishra, "Maximizing the power generation of a partially shaded PV array," *IEEE J. Emerg. Sel. Topics Power Electron.*, vol. 4, no. 2, pp. 626–637, Jun. 2016.

[22] A. S. Yadav, R. K. Pachauri, Y. K. Chauhan, S. Choudhury, and R. Singh, "Performance enhancement of partially shaded PV array using novel shade dispersion effect on magic-square puzzle configuration," *Sol. Energy*, vol. 144, pp. 780–797, Mar. 2017.

[23] S. Vijayalekshmy, G. R. Bindu, and S. R. Iyer, "A novel Zig-Zag scheme for power enhancement of partially shaded solar arrays," *Sol. Energy*, vol. 135, pp. 92–102, Oct. 2016.

[24] N. Belhaouas, M.-S.-A. Cheikh, P. Agathoklis, M.-R. Oularbi, B. Amrouche, K. Sedraoui, and N. Djilali, "PV array power output maximization under partial shading using new shifted PV array arrangements," *Appl. Energy*, vol. 187, pp. 326–337, Feb. 2017.

[25] B. Dhanalakshmi and N. Rajasekar, "Dominance square based array reconfiguration scheme for power loss reduction in solar PhotoVoltaic (PV) systems," *Energy Convers. Manage.*, vol. 156, pp. 84–102, Jan. 2018.

[26] D. S. Pillai, J. P. Ram, M. S. S. Nihanth, and N. Rajasekar, "A simple, sensorless and fixed reconfiguration scheme for maximum power enhancement in PV systems," *Energy Convers. Manage.*, vol. 172, pp. 402–417, Sep. 2018.

[27] I. Nasiruddin, S. Khatoon, M. F. Jalil, and R. C. Bansal, "Shade diffusion of partial shaded PV array by using odd-even structure," *Sol. Energy*, vol. 181, pp. 519–529, Mar. 2019.

[28] R. Pachauri, A. S. Yadav, Y. K. Chauhan, A. Sharma, and V. Kumar, "Shade dispersion-based photovoltaic array configurations for performance enhancement under partial shading conditions," *Int. Trans. Electr. Energy Syst.*, vol. 28, no. 7, p. e2556, Jul. 2018.

[29] A. Srinivasan, S. Devakirubakaran, and B. Meenakshi Sundaram, "Mitigation of mismatch losses in solar PV system–two-step reconfiguration approach," *Sol. Energy*, vol. 206, pp. 640–654, Aug. 2020.

[30] D. Yousri, T. S. Babu, E. Beshr, M. B. Eteiba, and D. Allam, "A robust strategy based on marine predators algorithm for large scale photovoltaic array reconfiguration to mitigate the partial shading effect on the performance of PV system," *IEEE Access*, vol. 8, pp. 112407–112426, 2020.

[31] D. Yousri, S. B. Thanikanti, K. Balasubramanian, A. Osama, and A. Fathy, "Multi-objective grey wolf optimizer for optimal design of switching matrix for shaded PV array dynamic reconfiguration," *IEEE Access*, vol. 8, pp. 159931–159946, 2020.

[32] S. R. Pendem, S. Mikkili, and P. K. Bonthagorla, "PV distributed-MPP tracking: Total-cross-tied configuration of string-integrated-converters to extract the maximum power under various PSCs," *IEEE Syst. J.*, vol. 14, no. 1, pp. 1046–1057, Mar. 2020.

[33] D. Yousri, D. Allam, and M. B. Eteiba, "Optimal photovoltaic array reconfiguration for alleviating the partial shading influence based on a modified Harris hawks optimizer," *Energy Convers. Manage.*, vol. 206, Feb. 2020, Art. no. 112470.

**MURUGESAN PALPANDIAN** received the B.E. degree in electrical and electronics engineering, the M.E. degree in power electronics and drives, and the Ph.D. degree from Anna University, Chennai, India, in 2006, 2009, and 2012, respectively. He is currently working as an Associate Professor with the Thamirabharani Engineering College, Tirunelveli, India. His current research interests include the solar PV systems, partial shading effects, and converters.

**DAVID PRINCE WINSTON** (Member, IEEE) received the B.E. degree in electrical and electronics engineering, the M.E. degree in power electronics and drives, and the Ph.D. degree from Anna University, Chennai, India, in 2006, 2008, and 2013, respectively. He is currently working as a Professor with the Department of Electrical and Electronics Engineering, Kamaraj College of Engineering and Technology, Madurai, India. He has published 35 research articles in several reputed international journals. His current research interests include solar PV, solar still, energy conservation in electric motor drives, power converters, power quality, and electric vehicles.

**BALACHANDRAN PRAVEEN KUMAR** received the B.E. degree in electrical and electronics engineering and the M.E. and Ph.D. degrees in power systems engineering from Anna University, Chennai, India, in 2014, 2016, and 2019, respectively. He is currently working as an Assistant Professor with the Department of EEE, Bharat Institute of Engineering and Technology, Hyderabad, India. His current research interests include solar photovoltaics, solar still, and renewable energy systems.

**CHERUKURI SANTHAN KUMAR** received the B.Tech. degree in electrical and electronics engineering from JNTUK, Kakinada, India, in 2009, the M.Tech. degree in power systems from ANU, Guntur, India, in 2012, and the Ph.D. degree in electrical and electronics engineering from JNTUK, in 2019. He is currently working as an Associate Professor and the Head of the Department with the Department of Electrical and Electronics Engineering, Lords Institute of Engineering and Technology, Hyderabad, India. His current research interests include solar PV systems, optimization of power systems, and hybrid energy systems.

**THANIKANTI SUDHAKAR BABU** (Senior Member, IEEE) received the B.Tech. degree from Jawaharlal Nehru Technological University, Anantapur, India, in 2009, the M.Tech. degree in power electronics and industrial drives from Anna University, Chennai, India, in 2011, and the Ph.D. degree from VIT University, Vellore, India, in 2017.

He is currently working as an Associate Professor with the Department of Electrical Engineering, Chaitanya Bharathi Institute of Technology (CBIT), Hyderabad, India. He has completed his Postdoctoral Researcher Fellowship from the Institute of Power Engineering, Universiti Tenaga Nasional (UNITEN), Malaysia. Before to that, he was worked as an Assistant Professor with the School of Electrical Engineering, VIT University. He has published more than 70 research articles in various renowned international journals. His research interests include the design and implementation of solar PV systems, renewable energy resources, power management for hybrid energy systems, storage systems, fuel cell technologies, electric vehicles, and smart grids. He has been acting as an Associate Editor of *IET RPG*, IEEE Access, *ITEES* (Wiley), and *Frontiers in Energy Research*; the Section Editor of *Energies* and *Sustainability* (MDPI Publications); and a Reviewer of various reputed journals.

**HASSAN HAES ALHELOU** (Senior Member, IEEE) was a Ph.D. Researcher with the Isfahan University of Technology (IUT), Isfahan, Iran. He is currently with University College Dublin, Ireland. He is also a Faculty Member with Tishreen University, Latakia, Syria. He has published more than 130 research articles in high-quality peer-reviewed journals and international conferences. He has participated in more than 15 industrial projects. His major research interests include power systems, power system dynamics, power system operation, and control, dynamic state estimation, frequency control, smart grids, micro-grids, demand response, load shedding, and power system protection. He has also performed more than 600 reviews for high-prestigious journals, including IEEE Transactions on Industrial Informatics, IEEE Transactions on Industrial Electronics, *Energy Conversion and Management*, *Applied Energy*, and *International Journal of Electrical Power and Energy Systems*. He is included in the 2018 and 2019 Publons list of the Top 1% Best Reviewer and Researchers in the field of engineering. He was a recipient of the Outstanding Reviewer Award from *Energy Conversion and Management* journal in 2016, *ISA Transactions* journal in 2018, *Applied Energy* journal in 2019, and many other awards. He was a recipient of the Best Young Researcher in the Arab Student Forum Creative among 61 researchers from 16 countries at Alexandria University, Egypt, in 2011.

• • •